

Switching Droplet Positions by Concentration Gradients

Samuel Krüger,^{1,2,3} Christoph A. Weber,^{1,3,4} Jens-Uwe Sommer,^{2,5,3} and Frank Jülicher^{1,3}

¹*Max Planck Institute for the Physics of Complex Systems,
Nöthnitzer Str. 38, 01187 Dresden, Germany*

²*Leibniz-Institut für Polymerforschung, Dresden 01069, Germany*

³*Center for Advancing Electronics Dresden cfAED, Dresden, Germany*

⁴*Division of Engineering and Applied Sciences,
Harvard University, Cambridge, MA 02138, USA*

⁵*TU Dresden, Institute for Theoretical Physics, Zellescher Weg 17, 01069 Dresden*

Abstract

Here we investigate how droplet position can be controlled using concentration profiles of a regulator that influences phase separation. We consider a mean field model of a ternary mixture where a concentration gradient of a regulator is imposed by an external potential. We show that novel first order phase transition exists that controls droplet position in a discontinuous manner. Such a droplet switch in concentration gradients could be relevant for the spatial organization of biological cells and provides a control mechanism for droplets in microfluidic systems.

PACS numbers: 47.55.D-, 64.75.Xc, 87.15.Zg

When a complex mixture separates into two coexisting phases, an inhomogeneous state emerges where droplets coexist with a surrounding fluid [1, 2]. Such droplets can be transported in a fluid flow or move subject to external forces such as gravity. A key question is whether droplets can be positioned using chemical cues such as concentration gradients of a molecular species in the solution. The chemical positioning of droplets has been suggested to be important for the spatial organisation of biological cells by positioning membraneless compartments [3–5]. Chemical control of droplet position also opens interesting possibilities for the control of droplets in microfluidic devices and in emulsions.

Here we propose a simple model to study the positioning of droplets. We describe phase separation of two components which are embedded in a concentration gradient of a further component that can affect phase separation. We consider the case where the concentration gradient is generated by an external field. The spatial distributions of all three concentration profiles are numerically calculated by minimizing a mean field free energy. We find that as a function of an interaction parameter the droplet position switches discontinuously from a position in the region of large regulator concentration (correlated state) to the region of low regulator concentration (anti-correlated). This switching of position corresponds to a novel first order phase transition at which an order parameter undergoes a jump (Fig. 1(a,b)). Our work shows that a switch-like change of the position of droplets can be realized by a discontinuous phase transition in systems where phase separation is combined with a regulator gradient.

Spatial regulation of phase separation. In our model for spatial regulation of phase separation we consider three components [6]: two components which can demix from each other, A and B , and a regulator R that interacts with these components. Demixing and interactions with the regulator are described by the Flory-Huggins free energy density for three components [7, 8]:

$$\begin{aligned}
 f(\phi_A, \phi_R) = \frac{k_b T}{\nu} & \left[\phi_R \ln \phi_R + \phi_A \ln \phi_A + \phi_B \ln \phi_B \right. \\
 & + \chi_{AR} \phi_A \phi_R + \chi_{RB} \phi_R \phi_B + \chi_{AB} \phi_A \phi_B \\
 & \left. + \frac{\kappa_R}{2} |\nabla \phi_R|^2 + \frac{\kappa_A}{2} |\nabla \phi_A|^2 + (U/k_b T) \phi_R \right].
 \end{aligned} \tag{1}$$

We consider the incompressible system in which the molecular volumes are equal to ν and $\phi_B = 1 - \phi_R - \phi_A$. The logarithmic contributions correspond to the mixing entropy, while

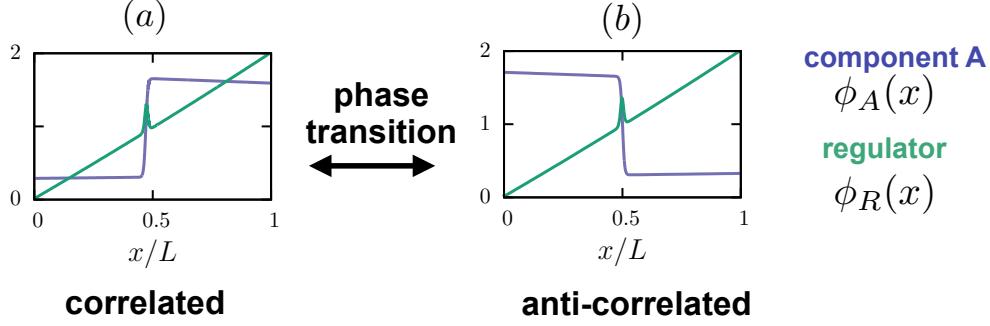


FIG. 1. Spatial regulation of phase separation by a discontinuous phase transition. (a,b) The regulator (green) forms a gradient due to an external potential. Depending on the interactions with the regulator the spatial distribution of e.g. component A (purple; component B behaves oppositely) switches from a spatially correlated (a) to an anti-correlated (b) distribution with respect to the regulator. The switch corresponds to a discontinuous phase transition.

the second line in Eq. (1) describes the molecular interactions between the components; χ_{ij} is the interaction parameter between component i and j . The gradient terms represent contributions to the free energy associated with spatial inhomogeneities. They introduce two length scales, $\sqrt{\kappa_A}$ and $\sqrt{\kappa_R}$. The regulator R is subject to an external field described by a position-dependent potential $U(x)$. For simplicity we consider in the following a one-dimensional system and choose a potential of the form $U(x) = -k_b T \ln(1 + s(2x - L))$, where $s > 0$ characterizes the slope of the potential and its inverse is a third length scale in our model. Note that in the absence of A and for $\phi_R \ll \phi_B$, $\phi_R(x)$ attains a concentration profile that is linear in space with a slope s . We consider a finite system of size L and two type of boundary conditions: (i) Neumann boundary conditions, $\phi'_i(0) = \phi'_i(L) = 0$, for all fields, where the primes denote spatial derivatives, and (ii) periodic boundaries with $\phi_i(0) = \phi_i(L)$ and $\phi'_i(0) = \phi'_i(L)$. The conditions (i) imply that there is no explicit energetic bias to wet or dewet the boundary, but the presence of the boundary enforces the slopes of the concentration profiles close to the boundary. In contrast, the periodic conditions (ii) allow to study the system in the absence of boundaries.

Stationary concentration profiles. To calculate the stationary and spatially dependent solutions of $\phi_A(x)$ and $\phi_R(x)$ we minimize the total free energy of the system,

$$F[\phi_A(x), \phi_R(x)] = \int_0^L dx f(\phi_A(x), \phi_R(x), x). \quad (2)$$

Due to particle number conservation, two constraints are imposed for the minimization that impose that each field ($i = A, R$) obeys $\bar{\phi}_i = L^{-1} \int_0^L dx \phi_i(x)$, where $\bar{\phi}_i$ are the average volume fractions and $\bar{\phi}_B = 1 - \bar{\phi}_A - \bar{\phi}_R$. Variation of the free energy Eq. (2) with the constraints of particle number conservation implies ($i = A, R$):

$$0 = \int_0^L dx \left(\frac{\partial f}{\partial \phi_i} - \frac{d}{dx} \frac{\partial f}{\partial \phi'_i} + \lambda_i \right) \delta \phi_i + \kappa_i \delta \phi_i \phi'_i \Big|_0^L, \quad (3)$$

where λ_R and λ_A are Lagrange multipliers, and the prime denotes a derivative with respect to x . The boundary terms vanish for both, Neumann and periodic boundary conditions. Using the explicit form of the free energy density (Eq. (1)), the Euler-Lagrange equations read:

$$0 = \ln \left(\frac{\phi_R}{1 - \phi_R - \phi_A} \right) + \chi \phi_A - 2 \chi_{RB} \phi_R + \chi_{RB} + \lambda_R - \ln(1 + s(2x - L)) - \frac{\kappa_R}{L^2} \phi_R'', \quad (4a)$$

$$0 = \ln \left(\frac{\phi_A}{1 - \phi_R - \phi_A} \right) + \chi \phi_R - 2 \chi_{AB} \phi_A + \chi_{AB} + \lambda_A - \frac{\kappa_A}{L^2} \phi_A''. \quad (4b)$$

Here, we defined $\chi = \chi_{AR} - \chi_{AB} - \chi_{RB}$ and rescaled length $x \rightarrow x L$. We solve Eqs. (4) numerically using a finite difference solver (bvp4c in MATLAB [9]). As control parameters we consider the three interaction parameters χ_{AR} , χ_{AB} and χ_{RB} , the slope of the external potential s and the mean volume fraction of A -material, $\bar{\phi}_A$. The mean regulator material is fixed to $\bar{\phi}_R = 0.02$ in all presented studies. Moreover, we focus on the limit of strong phase segregation where the interfacial width is small compared to the system size, i.e. $\sqrt{\kappa_i} \ll L$. In this limit, we verified that our results depend only weakly on the specific values of κ_i [10].

Discontinuous phase transition of droplet position. Solving Eqs. (4) with Neumann boundary conditions (i), we find two spatially inhomogeneous solutions for component A , which we denote $\phi_A^l(x)$ and $\phi_A^r(x)$, and the two corresponding solutions for the regulator component R , are denoted $\phi_R^l(x)$ and $\phi_R^r(x)$ (the profile of B follows from volume conservation). The phase separating material A is either accumulated close to the right boundary of the system ($\phi_R^r(x)$ and $\phi_A^r(x)$) and correlated with the concentration of the regulator material (Fig. 1(a)), or it is accumulated at the left ($\phi_R^l(x)$ and $\phi_A^l(x)$) and anti-correlated with the regulator (Fig. 1(b)). Upon varying the interaction parameters χ_{RB} in Fig. 7(a,b), the free

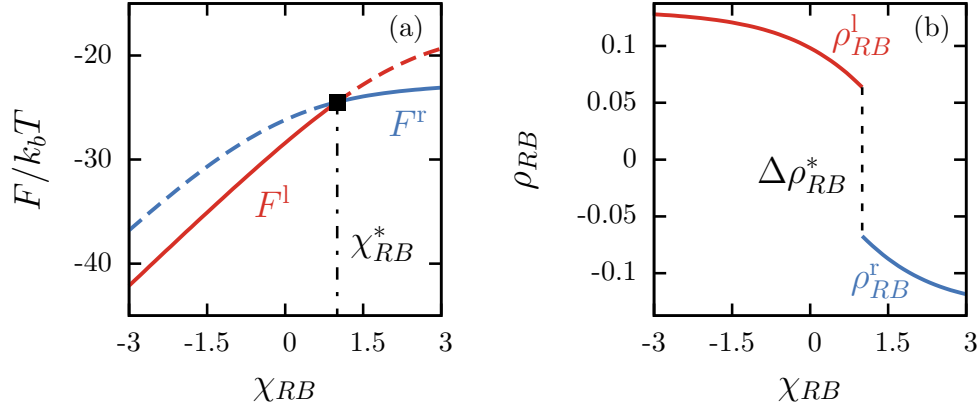


FIG. 2. Discontinuous phase transition. (a) Free energy F (Eq. (2)) as a function of the R - B interaction parameter χ_{RB} . F^l and F^r are the free energies of the correlated and anti-correlated stationary solution with respect to the regulator gradient, respectively (Fig. 1(a,b)). Lines are dashed when solutions are metastable. At χ_{RB}^* , F^l and F^r intersect and the solution of lowest free energy exhibits a kink. This shows that the transition between correlation and anti-correlation is a discontinuous phase transition. (b) The order parameter ρ^{RB} (Eq. (5)) jumps at χ_{RB}^* by a value of $\Delta\rho_{RB}^*$. The transition point χ_{RB}^* does not depend on the slope of the regulator s , while χ_{RB}^* increases linearly with s (see Supplemental Material [11], IV) Parameters: $\chi_{AB} = 4$, $\chi_{AR} = 1$, $\bar{\phi}_A = 0.5$, $\bar{\phi}_R = 0.02$, $\kappa_R/L^2 = 7.63 \cdot 10^{-5}$, $\kappa_A/L^2 = 6.10 \cdot 10^{-5}$, $Ls = 0.99$. For plotting, $\nu = L/256$ was chosen.

energies of the correlated and the anti-correlated states, $F^r = F[\phi_A^r, \phi_R^r]$ and $F^l = F[\phi_A^l, \phi_R^l]$, are different. They intersect at one point $\chi_{RB} = \chi_{RB}^*$ (Fig. 7(a)). At this point the lowest free energy exhibits a kink, which means that the system undergoes a discontinuous phase transition when switching from the spatially anti-correlated ('left') to the spatially correlated ('right') solution with respect to the regulator. A set of order parameters suitable to study this phase transition are

$$\begin{aligned} \rho_{ij} &= (k_b T L \mathcal{N}_{ij} / \nu)^{-1} \frac{d}{d\chi_{ij}} [F(\phi_i(x), \phi_j(x)) - F(\bar{\phi}_i, \bar{\phi}_j)] \\ &= \mathcal{N}_{ij}^{-1} \int_0^L dx (\phi_i(x) \phi_j(x) - \bar{\phi}_i \bar{\phi}_j), \end{aligned} \quad (5)$$

where the squared normalization $\mathcal{N}_{ij}^2 = \text{Var}(\phi_i^\Theta) \text{Var}(\phi_j^\Theta)$ with $\text{Var}(\phi_i) = \int_0^L dx (\phi_i^2(x) - \bar{\phi}_i^2)$, denoting the variance and $\phi_i^\Theta(x) = \Theta(L\bar{\phi}_i - x)$, where $\Theta(\cdot)$ denotes the heaviside step function. This normalization ensures that $-1 < \rho_{ij} < 1$ and $\rho_{ij} = \pm 1$ if $\phi_i(x) = \phi_i^\Theta(x)$.

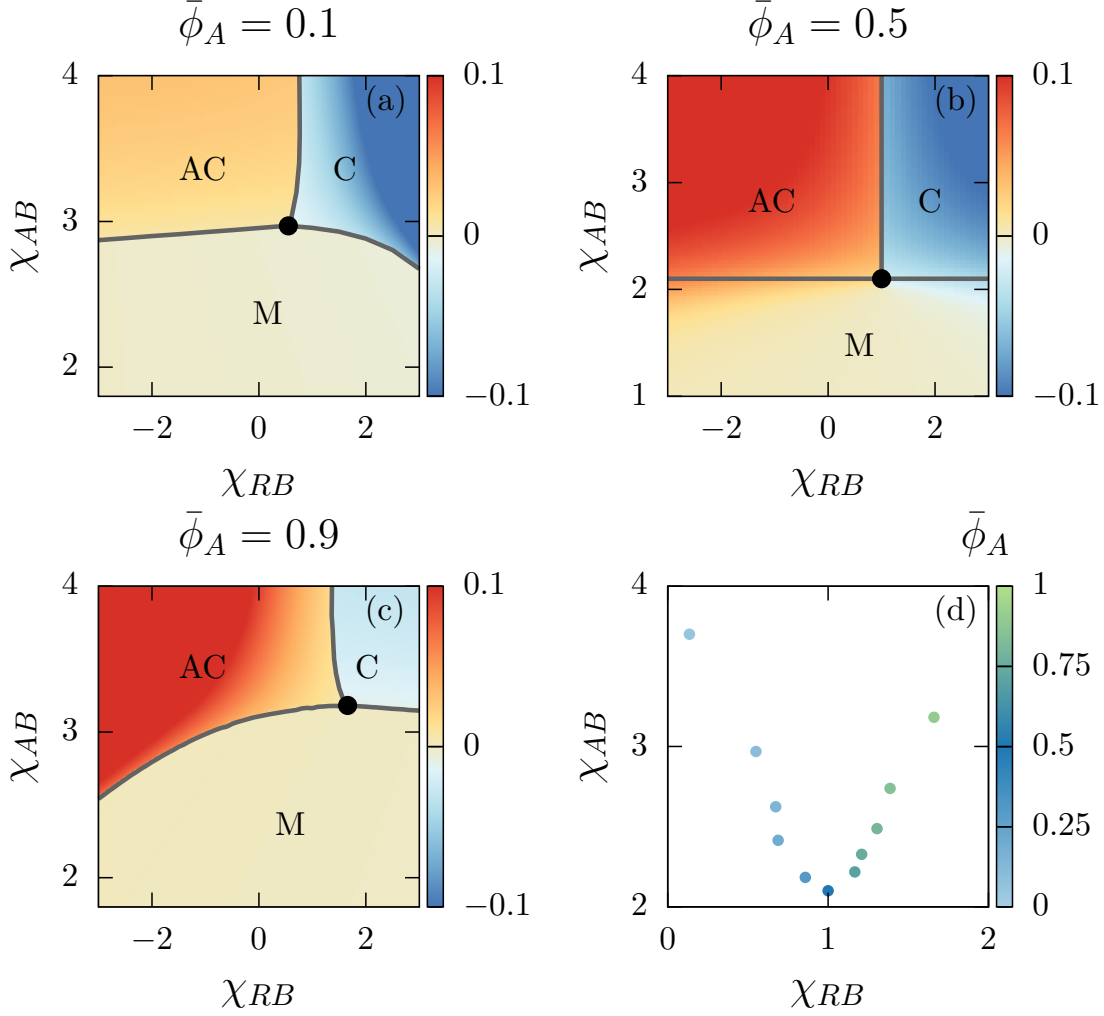


FIG. 3. Phase diagrams of our ternary model with spatial regulation. (a-c) Phase diagram for three volume fractions $\bar{\phi}_A = \{0.5, 0.1, 0.9\}$ and varying the interaction parameters χ_{AB} and χ_{RB} . The color code depicts the order parameter ρ_{BR} defined in Eq. (5). Component A is spatially correlated (C) with the regulator profile if $\rho_{BR} < 0$, and anti-correlated (AC) otherwise. When the system is mixed (M), $\rho_{BR} \approx 0$, and spatial profiles of all components are only weakly inhomogeneous (no phase separation). The solid black line in (a) is the transition line between A and AC calculated with the ansatz Eq. (7) using condition (6). The triple point (black dot) corresponds to the point in the phase diagrams where the three regions meet and the three free energies are equal. (d) Triple point for different $\bar{\phi}_A$ values (color code). Parameters: $\chi_{AR} = 1$, $\bar{\phi}_R = 0.02$, $\kappa_R/L^2 = 7.63 \cdot 10^{-5}$, $Ls = 0.99$, $\nu = L/256$.

The derivative of the free energy with respect to the interaction parameter χ_{ij} generates

the covariance between the spatially dependent fields $\phi_i(x)$ and $\phi_j(x)$. If the fields are spatially correlated, $\rho_{ij} > 0$, and if they are anti-correlated, $\rho_{ij} < 0$. For homogenous fields with $\phi_i(x) = \bar{\phi}_i$, $\rho_{ij} = 0$. Varying the interaction parameter χ_{RB} (Fig. 7(b)), the order parameters ρ_{RB} and ρ_{RA} jump at the threshold value χ_{RB}^* , while in the absence of a regulator gradient ($s = 0$), they change smoothly. The jump of both order parameters in the presence of a regulator gradient indicates that the spatial correlation of A and B to R changes abruptly, which is expected in case of a first order phase transition.

Phase diagrams. By means of the order parameter ρ_{RB} (Eq. (5)) we can now discuss the phase diagrams as a function of the interaction parameters for different volume fractions of the demixing material, $\bar{\phi}_A$. We find three regions (Fig. 3(a-c)): (i) A mixed region (M), where volume fraction profiles are only weakly inhomogeneous and no droplets occur. In addition, there are two regions, (C) and (AC), where components A and B phase separate and A is spatially correlated or anti-correlated with the regulator R , respectively. There exists a triple point where all three states have the same free-energy. For $\bar{\phi}_A = 1/2$, the shape of the transition line between correlated and anti-correlated states is straight and χ_{RB}^* independent of χ_{AB} (Fig. 3(a-d)). A decrease of $\bar{\phi}_A$ favors a correlated state and leads to an increase of the corresponding region while the region corresponding to an anti-correlated state in the phase diagram enlarges for decreasing $\bar{\phi}_A$. The transition line to the mixed states is horizontal for $\bar{\phi}_A = 1/2$ (Fig. 3(b)). For both, larger and smaller $\bar{\phi}_A$ -values, it becomes curved and moves towards larger χ_{AB} interaction parameters. This behaviour can be qualitatively understood by the upshift of the demixing threshold χ_{AB} once $\bar{\phi}_A$ deviates from $1/2$, as known for binary systems. Since the concentration of R is small here, this analogy provides a good approximation ($\bar{\phi}_R \rightarrow 0$ in Eq. (1)). Both trends explain the parabolic shape of the positions of the triple point in the phase diagrams when $\bar{\phi}_A$ is varied (Fig. 3(d)).

The transition line in the phase diagrams between the correlated and anti-correlated solution as a function of the interaction parameters can be estimated analytically. In the absence of a regulator gradient ($s = 0$), the free energies of both solutions are the same for all interaction parameters for which phase separation occurs. In the presence of a regulator gradient, however, the free energies corresponding to the correlated and the anti-correlated solutions are unequal for most points in the phase diagram. The reason is that the external potential $U(x)$ forces the regulator to form a gradient, and thus the interactions with the

regulator lead to different free energies of the correlated and anti-correlated states. Only along the transition line between both states the free energies equal:

$$\Delta F = F[\phi_A^r, \phi_R^r] - F[\phi_A^l, \phi_R^l] = 0. \quad (6)$$

This condition allows us to estimate the dependence of the transition lines as a function of the interactions parameters and the slope of the potential. To estimate ΔF we parametrize the profiles of the stationary solutions $\phi_A^{r,l}$ and $\phi_R^{r,l}$ using physical assumptions that are in agreement with our numerical results. First we idealize the already narrow interface of the demixed component ϕ_A as sharp. Since the regulator is maintained by the external potential, we find $\phi_R^r(x) \simeq \phi_R^l(x)$ close to the transition line. Thus we use the one profile, denoted as $\phi_R(x)$, for both regulator states. In addition, we approximate the regulator profile as linear function with slope m , neglecting spatial non-linearities that can be seen in Fig. 1(a,b). The low volume fractions outside the droplet of the demixed binary A - B system are approximated as constant values $\tilde{\phi}_{\text{out}}$. The larger volume fraction (inside) shows a weak linear spatial profile (Fig. 1(a,b)). For most parameters, the volume fraction inside the droplet can be well described as $\phi_{\text{in}}(x) = \tilde{\phi}_{\text{in}} - \phi_R(x)$, where $\tilde{\phi}_{\text{in}}$ is the constant volume fraction inside the droplet of the binary A - B mixture (see Supplemental Material [11], III). The approximated profiles are:

$$\phi_A^l(x) = \left[\phi_{\text{in}}(x) - \tilde{\phi}_{\text{out}} \right] \Theta(\epsilon_l - x) + \tilde{\phi}_{\text{out}}, \quad (7a)$$

$$\phi_A^r(x) = \left[\phi_{\text{in}}(x) - \tilde{\phi}_{\text{out}} \right] \Theta(\epsilon_r - L + x) + \tilde{\phi}_{\text{out}}, \quad (7b)$$

$$\phi_R(x) = m(x - L/2) + \bar{\phi}_R. \quad (7c)$$

The conservation of A determines the domain sizes $\epsilon_{l,r}$ of the phase separated region (see Supplemental Material [11], II). To calculate ΔF defined in Eq. (6) the free energy density Eq. (1) is integrated in the domain $[0, L]$ using the approximations Eqs. (7), giving

$$\Delta F = \frac{k_b T}{\nu} \frac{\chi_{RB} - \chi_{AR}}{12} m \mathcal{G}, \quad (8)$$

where the value \mathcal{G} depends only of the parameters of the simplified solutions (see Supplemental Material [11], II). Consistently, $\Delta F = 0$, if there is no regulator gradient ($m = 0$). In presence of a regulator gradient, $\Delta F = 0$ if $\chi_{RB}^* \simeq \chi_{AR}$, which defines the transition line between the correlated and anti-correlated solution obtained from the parametrized solutions

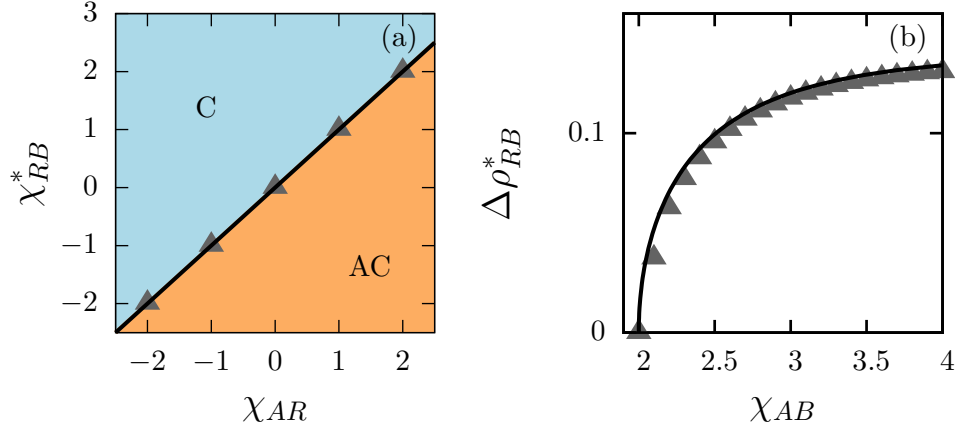


FIG. 4. Phase diagrams and order parameters estimated by ansatz Eq. (7). (a) The transition between spatial correlation (C) and anti-correlation (AC) of the distribution of component A with respect to the regulator in the χ_{AR} - χ_{RB} -plane. Parameters: $\chi_{AB} = 4$, $\bar{\phi}_A = 0.5$, $\bar{\phi}_R = 0.02$, $\kappa_R/L^2 = 7.63 \cdot 10^{-5}$, $\kappa_A/L^2 = 6.10 \cdot 10^{-5}$, $Ls = 0.99$, $\nu = L/256$. (b) Jump of the order parameter at the transition point, $\Delta \rho_{RB}^*$, as a function of the interaction parameter χ_{AB} . Additionally to the parameters of (a), $\chi_{AR} = 1$ and $\chi_{RB} = 1$. The black line in (a) and (b) shows the result obtained from using Eq. (7); the triangles are numerical results from the minimization of Eq. (2).

Eqs. (7). This prediction is in very good agreement with our numerical results for $\bar{\phi}_A \simeq 1/2$; see black lines in Fig. 3(a) and Fig. 4(a). By means of the Ansatz given in Eqs. (7) we can also analytically estimate how the jump of the order parameter $\Delta \rho_{RB}^*$ (definition see Fig. 7(b)) at the transition point depends on the model parameters. In particular we find that $\Delta \rho_{RB}^*$ obtained by this approximation as a function of the slope of the regulator (not shown) and the interaction parameter χ_{AB} (Fig. 4(b)) almost perfectly describe the data obtained from the numerical minimization of the free energy. This shows that the proposed parametrization of the stationary solutions represents a good approximation. The positioned and phase separated profiles have a sharp interface and the volume fraction inside has a weak linear slope that is mainly determined by volume exclusion with the regulator.

The phase diagrams depend on the boundary conditions rising the question whether the boundary play a key role for the existence of the phase transition. To this end we considered a periodic system without boundaries. We find that a first order transition of droplet position also exists for in the absence of boundaries (see Supplemental Material [11], I). Thus the transition is not induced by boundaries as for example in the case of wetting

transitions [12–14].

Our work reports a novel discontinuous phase transition, which can occur in demixing systems in the presence of a regulator gradient that affects phase separation. The phase transition switches between two stationary inhomogeneous profiles of phase separated material, which either spatially correlates or anti-correlates with the regulator gradient. The phase transition reported here arises from an interplay between the regulator profile and phase separation. The local regulator concentration lifts the energetic degeneracy in droplet position and leads to two coexisting stationary states with different droplet position. This discontinuous switching of phase separation predicted here could be tested experimentally. For example, soluble salt compounds of high magnetic susceptibility can be used to create and control concentration gradients via the application of a magnetic field [15]. Introducing components that phase separate in a salt dependent manner allows the observation of phase separation in a regulator gradient. The positional switching of droplets could be triggered by changing the concentrations of the phase separating material or components that influence the interaction parameters. The systems considered here could also be relevant for applications. Our phase transition of droplet position provides a novel mechanism to control and switch chemical environments in microfluidic devices.

We would like to thank Martin Elstner and Omar Adame for fruitful and stimulating discussions. This project was supported by the Center for Advancing Electronics Dresden (cfAED). Christoph A. Weber thanks the German Research Foundation (DFG) for financial support. Samuel Krüger and Christoph A. Weber contributed equally to this work.

-
- [1] A. Bray, *Advances in Physics* **43**, 357 (1994).
 - [2] A. Onuki, *Phase transition dynamics* (Cambridge University Press, 2002).
 - [3] C. P. Brangwynne, *Soft Matter* **7**, 3052 (2011).
 - [4] A. A. Hyman, C. A. Weber, and F. Jülicher, *Annual review of cell and developmental biology* **30**, 39 (2014).
 - [5] C. P. Brangwynne, P. Tompa, and R. V. Pappu, *Nature Physics* **11**, 899 (2015).
 - [6] C. F. Lee, C. P. Brangwynne, J. Gharakhani, A. A. Hyman, and F. Jülicher, *Phys. Rev. Lett.* **111**, 088101 (2013).

- [7] P. J. Flory, The Journal of chemical physics **10**, 51 (1942).
- [8] M. L. Huggins, The Journal of Physical Chemistry **46**, 151 (1942),
<http://dx.doi.org/10.1021/j150415a018>.
- [9] J. Kierzenka and L. F. Shampine, ACM TOMS **27**, 299 (2001).
- [10] Following Ref. [16], we use the relation $\kappa_A = \chi_{AB}$, κ_R is kept constant.
- [11] See Supplemental Material for videos and more information at <http://....>
- [12] J. W. Cahn, The Journal of Chemical Physics **66**, 3667 (1977).
- [13] M. Moldover and J. W. Cahn, Science **207**, 1073 (1980).
- [14] D. Pohl and W. Goldburg, Physical Review Letters **48**, 1111 (1982).
- [15] M. Takayasu, R. Gerber, and F. Friedlaender, IEEE Transactions on Magnetics **19**, 2112 (1983).
- [16] S. A. Safran, *Statistical Thermodynamics of Surface, Interfaces and Membranes* (Addison–Wesley Publishing Company, 1994).

SUPPLEMENTAL MATERIAL

Discontinuous phase transition in a periodic domain

Here we discuss the results of the minimization of the free-energy (Eq. (3), main text) using periodic boundaries with $\phi_i(0) = \phi_i(L)$ and $\phi'_i(0) = \phi'_i(L)$. We find the same qualitative results as for Neumann boundary conditions. The two stationary solutions of different spatial correlation with respect to the regulator change at a certain value of the interaction by a discontinuous phase transition (Fig. 5). Therefore a boundary of the system is not a necessary requirement for the emergence of the novel discontinuous phase transition discussed in our manuscript.

Estimate of ΔF

The free energy difference between the two stationary solutions, ΔF , results from integration over the domain $[0, L]$ using the simplified solutions (Eqs. (7), main text):

$$\Delta F = \frac{k_b T}{\nu} \frac{\chi_{RB} - \chi_{AR}}{12} m \mathcal{G}, \quad (9)$$

where

$$\mathcal{G} = \left[12\epsilon_l (L - \epsilon_l) \left(2\tilde{\phi}_{\text{out}} + 2\bar{\phi}_R - 1 \right) + 3(L - 2\epsilon_l) \left(m(L - 2\epsilon_l) + 4\tilde{\phi}_{\text{out}} + 2\bar{\phi}_R - 2 \right) \Delta\epsilon \right] \quad (10)$$

and

$$\epsilon_l = \frac{-2 - Lm + 4\tilde{\phi}_{\text{out}} + 2\bar{\phi}_R}{2m} + \frac{\sqrt{8Lm \left(\tilde{\phi}_{\text{out}} - \bar{\phi}_A \right) + \left(2 + Lm - 4\tilde{\phi}_{\text{out}} - 2\bar{\phi}_R \right)^2}}{2m}, \quad (11)$$

$$\epsilon_r = \frac{-2 + Lm + 4\tilde{\phi}_{\text{out}} + 2\bar{\phi}_R}{2m} + \frac{\sqrt{8Lm \left(\bar{\phi}_A - \tilde{\phi}_{\text{out}} \right) + \left(-2 + Lm + 4\tilde{\phi}_{\text{out}} + 2\bar{\phi}_R \right)^2}}{2m}. \quad (12)$$

Here we substituted the interaction parameter between B and A by χ_{AB}^* , and truncated at $O(\Delta\epsilon)$ with $\Delta\epsilon = \epsilon_r - \epsilon_l$. Consistently, $\Delta F = 0$, if there is no regulator gradient ($m = 0$), and when phase separation is absent ($\epsilon_l = \epsilon_r = 0, L$). \mathcal{G} depends only of the parameters of the simplified solutions (see Eqs. (7), main text).

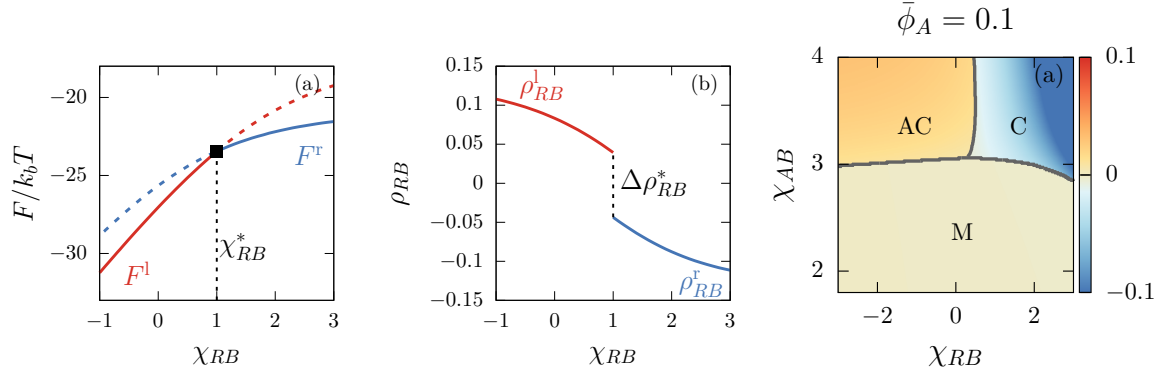


FIG. 5. Discontinuous phase transition in a periodic potential and periodic boundary conditions. (a) Free energy F as a function of the R - B interaction parameter χ_{RB} . F^l and F^r are the free energies of the correlated and anti-correlated stationary solution with respect to the regulator gradient, respectively. Lines are dashed when solutions are metastable. At χ_{RB}^* , F^l and F^r intersect and the solution of lowest free energy exhibits a kink. This shows that the transition between correlation and anti-correlation is a discontinuous phase transition. (b) The order parameter ρ^{RB} jumps at χ_{RB}^* by a value of $\Delta\rho_{RS}^*$. Parameters: $\chi_{AB} = 4$, $\chi_{AR} = 1$, $\bar{\phi}_A = 0.5$, $\bar{\phi}_R = 0.02$, $\kappa_R/L^2 = 7.63 \cdot 10^{-5}$, $\kappa_A/L^2 = 6.10 \cdot 10^{-5}$, $A = 0.5$. For plotting, $\nu = L/256$ was chosen. (c) Phase diagrams of our ternary model for spatial regulation in a periodic potential and periodic boundary conditions ($\bar{\phi}_A = 0.1$). The color code depicts the order parameter ρ_{BR} . Component A is spatially correlated (C) with the regulator profile if $\rho_{BR} < 0$, and anti-correlated (AC) otherwise. When the system is mixed (M), $\rho_{BR} \approx 0$, and spatial profiles of all components are only weakly inhomogeneous (no phase separation). The triple point (black dot) corresponds to the point in the phase diagrams where the three regions meet and the three free energies are equal. Parameters: $\chi_{AR} = 1$, $\bar{\phi}_R = 0.02$, $\kappa_R/L^2 = 7.63 \cdot 10^{-5}$, $A = 0.5$, $\nu = L/256$.

Comparison of simplified and full numerical solution

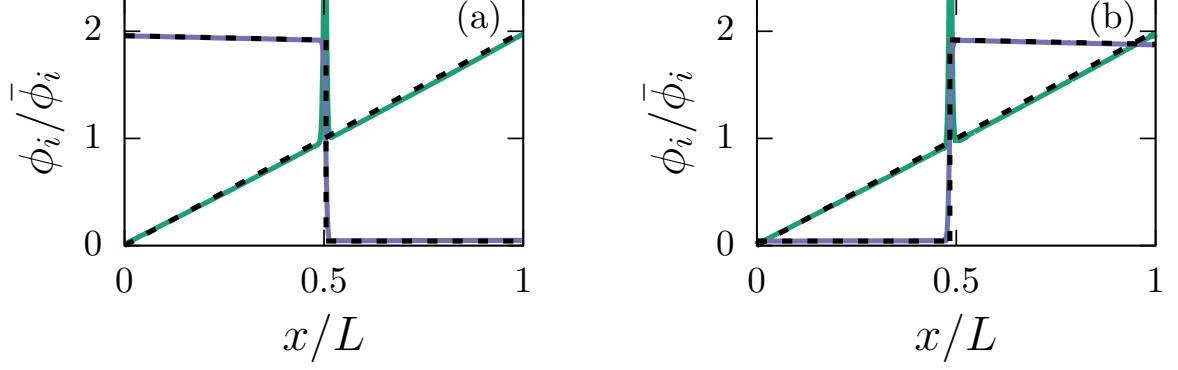


FIG. 6. (a) Anti-correlated profile and (b) Correlated profile close to the correlated-anti-correlated transition line. The dashed black lines depict the simplified profiles (Eqs. (7), main text) used in the analytic calculation of the free-energy difference between the free-energies of the two stationary solutions, ΔF . The peak of the regulator at the droplet interface is neglected in the analytical ansatz. Fixed parameters: $\chi_{AB} = 4$, $\chi_{AR} = 1$, $\chi_{RB} = 1$, $\bar{\phi}_R = 0.02$, $\phi_A = 0.5$, $\kappa_R/L^2 = 7.63 \cdot 10^{-5}$, $\kappa_D/L^2 = 6.10 \cdot 10^{-5}$, $Ls = 0.99$, $\nu = L/256$.

Transition point is independent of the regulator gradient

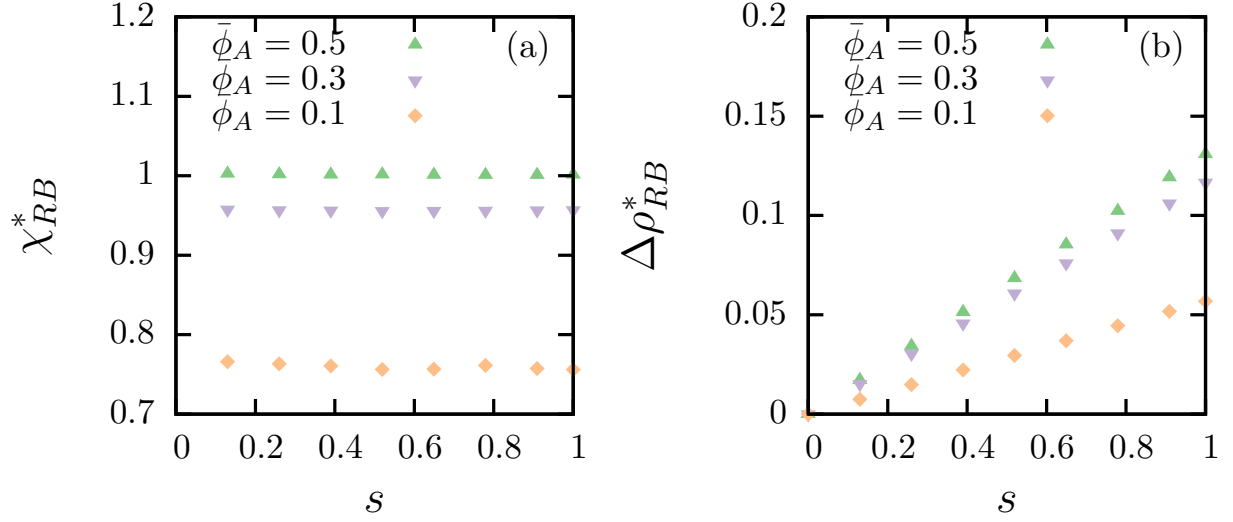


FIG. 7. (a) The transition point is independent on the slope of the regulator gradient s . (b) The jump of the order parameter at the transition point linearly increases with the slope of the gradient s . The slope of this linear dependence is influenced by $\bar{\phi}_A$. Fixed parameters: $\chi_{AB} = 4$, $\chi_{AR} = 1$, $\bar{\phi}_R = 0.02$, $\kappa_R/L^2 = 7.63 \cdot 10^{-5}$, $\kappa_D/L^2 = 6.10 \cdot 10^{-5}$, $\nu = L/256$.